



# Prediction of mechanical properties of zinc alloy based on machine learning algorithm

Kairan Yang<sup>1</sup>, Gulisitan Yisimayili<sup>2</sup>, Junyu Yue<sup>3\*</sup>

<https://doi.org/10.64486/m.65.1.4>

<sup>1</sup> School of Software, Xinjiang University, Urumqi, Xinjiang 830046, China [1522570489@qq.com](mailto:1522570489@qq.com)

<sup>2</sup> School of Economics and Management, Xinjiang University, Urumqi, Xinjiang 830046, China [960257894@qq.com](mailto:960257894@qq.com)

<sup>3</sup> School of Computing Science and Technology, University of Chinese Academy of Sciences, Beijing 101408, China

\* Correspondence: [yuejunyu21@mails.ucas.ac.cn](mailto:yuejunyu21@mails.ucas.ac.cn)

*Type of the Paper:* Article

*Received:* July 12, 2025

*Accepted:* August 22, 2025

**Abstract:** As a medical implant material, zinc alloys need to have high strength and sufficient hardness to support bone regeneration. Therefore, it is important to clearly define the design criteria for zinc alloys that meet the mechanical property requirements of degradable medical implants. In this work, mechanical property data of Zn-Mg-Mn alloys were obtained through experimental research and literature collection. A performance-oriented machine learning (ML) model was used to predict the compressive yield strength and hardness of Zn-Mg-Mn alloys with different element types, contents and alloy preparation processes, and then the influence of element types and contents on the microstructure and macroscopic mechanical properties of the material was explored. Based on the existing dataset, the model compared six different ML algorithms and identified the optimal prediction algorithm. To further verify the accuracy of the model's predictions, data outside the dataset were randomly selected for comparative analysis with the model results. The results showed that the prediction errors of the algorithm designed in this work for compressive yield strength and hardness were less than 2 % and 2.4 %, respectively.

**Keywords:** machine learning; zinc alloy; mechanical property prediction

## 1. Introduction

Compared with magnesium- and iron-based alloys, zinc-based alloys exhibit a more moderate corrosion rate, and their degradation products are fully absorbable and do not produce excessive hydrogen. Therefore, they are considered ideal alternative materials to magnesium-based alloys and iron-based alloys (1-4). Zinc-based alloys have been widely used in the biomedical field, especially in orthopedic regeneration and cardiovascular therapy (5-8). However, as biomedical implant materials, zinc-based alloys have poor mechanical properties that make it difficult for them to meet the requirements of most medical applications (9-13). Therefore, developing zinc alloys with excellent mechanical properties to expand their practicality and effectiveness as biomedical implants has become a core challenge facing clinical medicine and materials science.

Alloying is one of the main methods to improve the mechanical properties of zinc-based alloys (14). Elements such as Mg and Mn are added to zinc alloys because of their good biocompatibility. As an indispensable trace element for the human body, Mg plays a vital role in many cellular functions, including energy metabolism and cell proliferation, and does not produce toxic effects when implanted in the body. In addition, adding

Mg to the zinc matrix can effectively improve its mechanical properties. Studies have shown that adding 4 % Mg (mass fraction, same below) can significantly improve the compressive strength, increasing it by 257 MPa compared with pure Zn. Researchers have greatly improved the mechanical properties of 300 MPa-grade Zn-Mn-Mg alloys through microalloying design. The results showed that the tensile Zn-0.6Mn-0.06Mg and Zn-0.8Mn-0.05Mg alloys both exhibit high comprehensive mechanical properties, with a yield strength of (313-324) MPa, an ultimate tensile strength of (345-356) MPa, and an elongation at failure of (20-28) %. In addition, as a non-toxic alloying element, Mn can purify harmful impurities such as Fe and form an MnO film, which has a significant effect on the mechanical properties of zinc alloys. Relevant scholars studied the effect of adding different Mn contents (0.2 %, 0.4 % and 0.6 %) on the microstructure and mechanical properties of extruded Zn-Mn alloys, and found that after adding Mn, the elongation of the alloy increased significantly from 48 % to 71 %, but the compressive strength decreased slightly with increasing Mn content. Li et al. studied the effect of trace Mn alloying on the high-temperature compression behavior of pure Zn, and found that the addition of Mn greatly improved the high-temperature strength of pure Zn (14, 15). Its peak stress at 300 °C/0.1 s<sup>-1</sup> was 46 MPa, and it increased to 84 MPa after adding 0.8 % Mn. In summary, Mg and Mn have shown great potential for improving the mechanical properties of zinc alloys. By adding appropriate amounts of Mg and Mn to zinc alloys, their applicability in biomedical applications can be effectively improved.

Machine learning (ML), as a data-driven method, is an effective means of reducing the number of experimental and computational samples required (16-18). Numerous studies have shown that ML methods such as artificial neural networks, random forests and the extreme gradient boosting (XGBoost) algorithm can successfully optimize the design of material properties, accelerate the materials design process, and are suitable for predicting material properties and exploring new materials. Researchers have used machine learning methods to predict the compressive yield strength and corrosion rate of Mg alloys, and found that Zn has a key influence on both (19-21). They also proposed a composition design guide for medical Mg implants to meet the requirements of strength and corrosion rate, i.e., the ultimate compressive strength of magnesium alloys should reach or exceed 240 MPa, and the in vitro corrosion rate should be controlled below 1 mm/a. However, there is a relative lack of systematic research on machine-learning-guided zinc-alloy composition design and processing methods, making it difficult to fully evaluate the effectiveness and applicability of machine learning for zinc-alloy performance design (22-24).

To address this research gap, this study used six ML algorithms to predict the effects of alloying elements and processing routes on the compressive yield strength and microhardness of zinc alloys, and identified the best-performing model. A convolutional neural network (CNN) was used to guide alloy parameter design. This work provides more accurate and efficient guidance for subsequent optimization of alloy performance.

## 2. Materials and methods

### 2.1. Materials

Three kinds of metal powders, namely Zn, Mg and Mn powders, were selected and used to prepare Zn-Mg-Mn alloy. Table 1 shows the parameters of the alloy powders. An aliquot of the alloy powder was examined using a JSM-7800F scanning electron microscope (SEM) to assess particle size and morphology. Zn powder consisted of spherical, smooth particles with sizes < 30 µm; Mg powder had spherical, rough particles with a maximum size of 40 µm; Mn powder had irregular particles with sharp protrusions and a maximum size of 30 µm.

**Table 1.** Alloy powder parameters

Powder	Purity / %	Melting point / °C
Zn	99	419.5
Mg	99.9	648.9
Mn	99.9	1244

## 2.2. Material preparation

Zinc alloys with different element ratios were prepared by powder metallurgy. First, twenty powder mixtures with different ratios were weighed (50 g each) with an FA2004 electronic balance covering Mg contents of 0 % to 3 % and Mn contents of 0 % to 4.2 %. The weighed powders were poured into a ZrO<sub>2</sub> ball-milling jar, evacuated, and placed in a planetary ball mill for ball milling. The ball milling time was 48 h, the speed was 205 r/min, and the ball-to-powder mass ratio was 16:1. An intermittent ball milling process was adopted, pausing the mill for 10 min after running for 30 min. The pressureless sintering temperature of the mixed powder was determined using a 1600HT differential scanning calorimeter (DSC) (Figures 1a and 1b). Then, the mold filled with Zn, Mg, and Mn powders was cold pressed at a load of 15 t using a CMT5305 universal testing machine and the load was maintained for 5 min. Subsequently, the pressed sample was placed in a vacuum sintering furnace and the zinc alloy was produced using a two-step sintering (TSS) technology. Figure 1c shows the sintering process curve of the Zn-Mg-Mn alloy. First, the cold-pressed sample was heated from room temperature to 250 °C at a heating rate of 5 °C/min and held at this temperature for 1.5 h. This step involved sintering at a lower temperature to eliminate pores between the powder particles and promote the transformation of the alloy from low densification to high densification, thereby making the microstructure more uniform. The second step involved heating to 400 °C at a heating rate of 4 °C/min and holding at this temperature for 2 h before cooling in the furnace. This step was involved sintering at a higher temperature to promote grain growth and powder coalescence, increase densification and thus improve the density of the alloy.

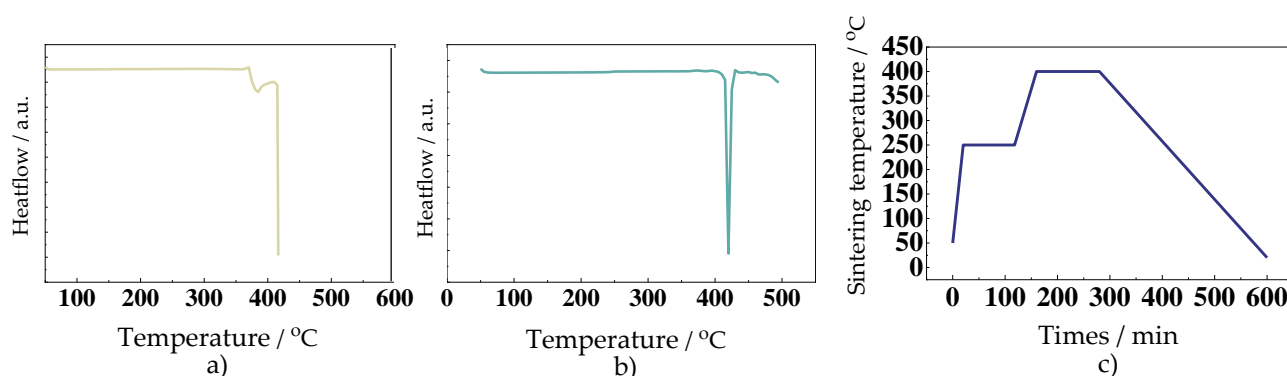


**Figure 1.** Differential scanning calorimetry (DSC) and sintering process curves of powder mixtures of a) Zn, b) Mg, and c) Mn

## 2.3. Mechanical testing

The test samples were cylinders with a diameter of 10 mm and a height of 15 mm. Each alloy was tested at least 3 times to obtain accurate compressive yield strength and the average and standard deviation of the data points were calculated. The samples were ground and polished using SiC sandpaper of grades 120, 400, 800, 1200, and 2000, and then ultrasonically cleaned for 5 min to remove surface contamination. The hardness of the zinc alloy was tested using an HV-100IS microhardness tester with a loading force of 200 gf and a loading time of 15 s. To ensure the accuracy of the measurement data, each sample was tested 10 times under the same conditions and the average of the remaining data was taken after discarding the highest and lowest values.

## 3. Results and discussion

### 3.1. Model construction

The data include the element types and contents, compressive yield strength and microhardness of Zn-Mg-Mn alloys prepared by powder metallurgy, as well as the element types and contents, compressive yield strength and microhardness of Zn-Mg-Mn alloys prepared by extrusion and casting collected from the literature. Mg and Mn contents and the preparation process are key parameters in alloy design, and these parameters are

closely related to the compressive yield strength of the alloys at room temperature. Based on this, 595 data points for 3 input variables (Mg, Mn and preparation process) and 2 output variables (compressive yield strength and hardness) were obtained.

This work uses six algorithms, including random forest (RF), logistic regression (LR), K-nearest neighbors (KNN), decision tree (DT), deep neural network (DNN) and convolutional neural network (CNN), to train the model. In order to reduce overfitting in nonlinear regression, the 10-fold cross-validation is used. The ratio of the training set to the test set is 8:2. Eighty percent of the 595 samples were randomly selected as the training set for model training, and 20 % of the data were used as the test set to verify the model's predictive ability. The final result was the average of 10 test results. The models used in this work have all been hyperparameter tuned, that is, the important hyperparameters in different model algorithms were selected and tuned. Based on the difference between the measured output and the predicted output, three common indicators were used to evaluate the performance of the regression model, namely: coefficient of determination ( $R^2$ ), root mean square error (RMSE) and mean absolute error (MAE).

### 3.2. Model training results

Figures 2 and 3 compare the predicted values of compressive yield strength and hardness from the six models with the corresponding experimental data. The experimental values and the predicted values lie roughly on the  $Y = X$  line, indicating that the model accurately predicts the mechanical properties of the alloy. It can be seen from the figures that the CNN model has the best fitting effect in the training stage. Figure 4 shows the average values of  $R^2$ , RMSE and MAE of the six machine learning models. Consistent with the fitting results in the model training stage, the CNN model has the best performance, and its  $R^2$ , RMSE and MAE values for the compressive yield strength model and the hardness model are 0.8694, 8.4356 and 15.3535, respectively. Among them, the  $R^2$  of the CNN model is greater than that of the other models, and the RMSE and MAE are lower than those of the other models. In summary, it is most appropriate to select the CNN model for predicting compressive yield strength and hardness.

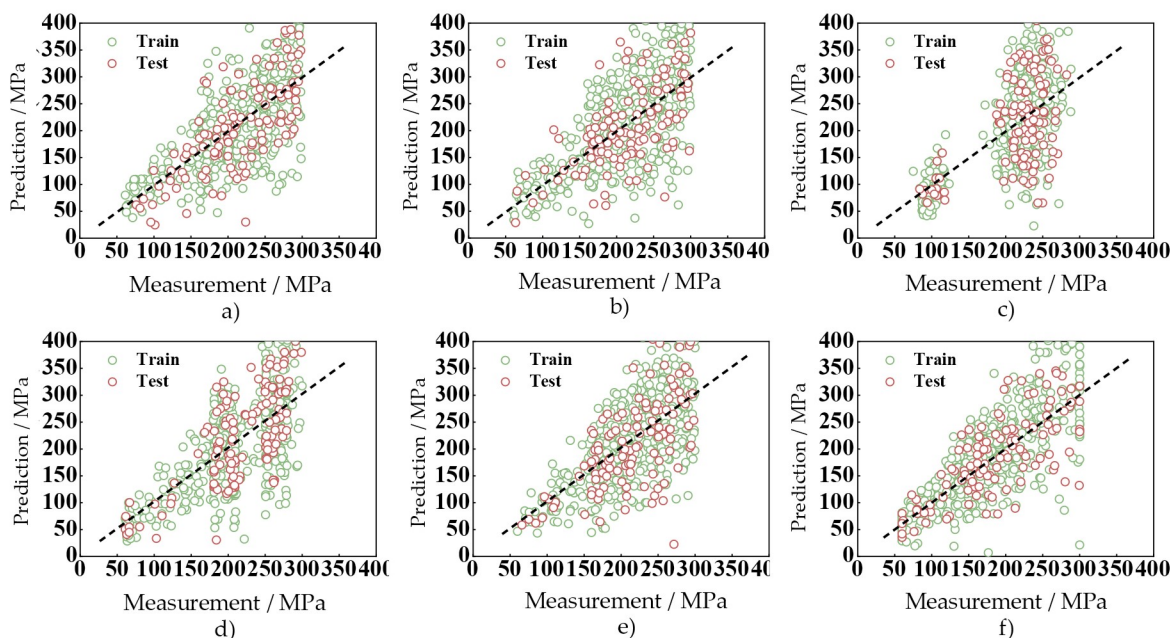


**Figure 2.** Experimental data of Zn-Mg-Mn alloy compressive strength and prediction results of six models. a) RF, b) LR, c) KNN, d) DT, e) DNN, f) CNN.



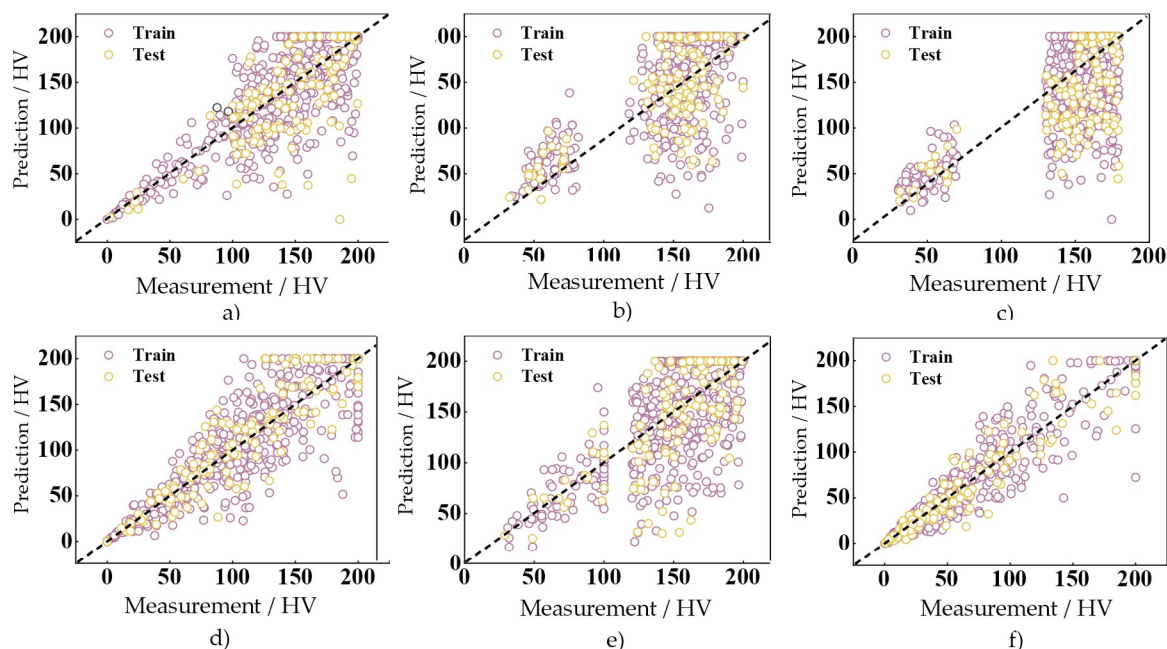


**Figure 3.** Experimental data of Zn-Mg-Mn alloy hardness and prediction results of six models.  
a) RF, b) LR, c) KNN, d) DT, e) DNN, f) CNN

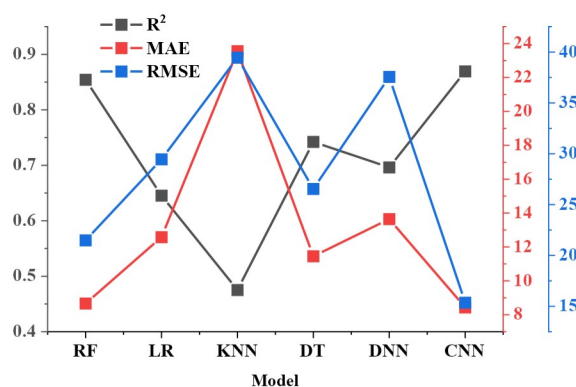


**Figure 4.** Comparison of the coefficient of determination (R<sup>2</sup>), root mean square error (RMSE) and mean absolute error (MAE) of the six models

### 3.3. Model validation

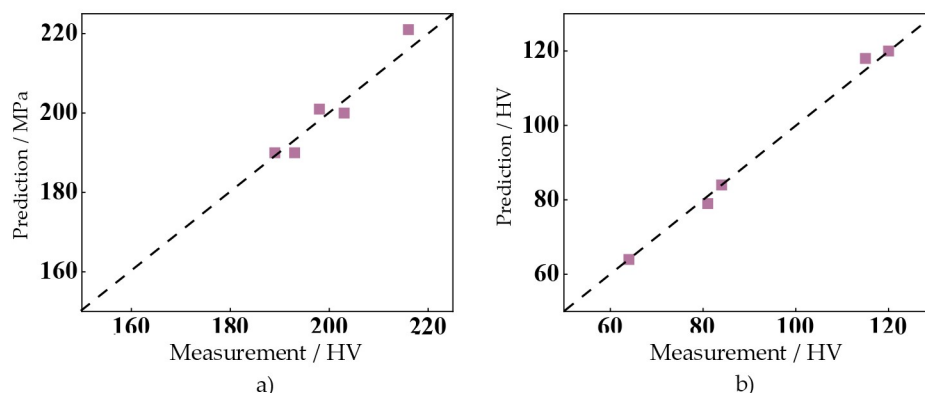
In order to further verify the accuracy of the CNN model in predicting the compressive yield strength and hardness of the zinc alloy, the predicted values are compared with the experimental data in the validation dataset. The validation dataset was obtained from experimental results and literature data, which were not included in the training dataset constructed above.

Table 2 shows the validation results of the dataset and experimental data (predicted and measured values of compressive yield strength and hardness). The results show that when the predicted value of the compressive yield strength of the alloy is 221 MPa, its maximum error is about 2 %, and when the predicted value of the hardness is 79 HV, its maximum error is about 2.4 %. The difference in error is small, indicating that the predicted value is in good agreement with the measured value. Figure 5 shows a comparison of the model predicted values and the measured values. It can be seen that the difference between the predicted values and the

measured values is small, and the degree of dispersion is low. Therefore, the CNN model has a high prediction accuracy for the compressive yield strength and hardness of the alloy.

**Table 2.** CNN model prediction model validation set

No .	Mg / %	Mn / %	Compressive strength / %	Hardness / HV
1	1.10	0.85	203/200	81/79
2	2.75	1.02	198/201	120/120
3	1.57	0.42	189/190	84/84
4	0.52	0.15	216/221	115/118
5	0.22	0.52	193/190	64/64



**Figure 5.** Comparison of the predicted values of a) compressive yield strength and b) hardness by the CNN model with the experimental values.

## 4. Conclusion

This work obtained 595 samples from experimental results and literature data. The large sample size improved the accuracy of data analysis. It also helped the model to generalize better and reduced the risk of over-fitting. Among the six models constructed, the CNN model performed best, with the highest coefficient of determination, the smallest root mean square error and mean absolute error. The compressive yield strength and hardness predicted by the KNN model were in good agreement with the experimental data, with errors less than 2 % and 2.4 % respectively. This verified that the machine learning prediction model in this work has high reliability.

**Acknowledgments:** The authors declare no conflicts of interest to disclose.

## References

- [1] E. AbdElrhieem, S. M. Abdelaziz, Y. F. Barakat, S. G. Mohamed, and H. I. Lebda, "A theoretical and experimental study on indentation creep with x-silica addition to an Al-8Zn composite alloy, based on Adaptive Neuro-Fuzzy Inference System (ANFIS)," *Materials Chemistry and Physics*, vol. 341, pp. 565-578, 2025., <https://doi.org/10.1016/j.matchemphys.2025.130937>
- [2] X. Chen, Y. Lu, M. Ning, X. Zhou, and J. Chen, "Tailoring microstructural evolution and fracture damage behavior of a Mg-Y-Zn alloy during hot tensile deformation," *Materials Science and Engineering: A*, vol. 871, 2023., <https://doi.org/10.1016/j.msea.2023.144857>

- [3] X. Chen, D. Wang, Q. Li, Y. Xiong, K. Tian, and P. Chen, "Hot compression behavior and microstructure evolution of Mg-Gd-Y-Zn-Zr alloy," *Journal of Materials Research and Technology*, vol. 30, pp. 755-768, 2024., <https://doi.org/10.1016/j.jmrt.2024.03.112>
- [4] M. Deif, H. Attar, M. Aljaidi, A. Alsarhan, D. Al-Fraihat, and A. Solyman, "Machine learning alloying design of bio-degradable zinc alloy for bone implants using XGBoost and Bayesian optimization," *Intelligent Systems with Applications*, vol. 27, pp. 1347-1358, 2025., <https://doi.org/10.1016/j.iswa.2025.200549>
- [5] F. O. Edoziuno, A. A. Adediran, P. O. Emerije, R. O. Akaluzia, and T.-C. Jen, "Development of lightweight, creep resistant Mg-Zn-Al alloys for automotive applications: Influence of micro-additions of quaternary elements," *Results in Engineering*, vol. 21, pp. 1283-1293, 2024., <https://doi.org/10.1016/j.rineng.2023.101632>
- [6] F. O. Edoziuno, P. O. Emerije, B. U. Odoni, R. O. Akaluzia, and N. C. Chukwurah, "Experimental analysis and response surface optimization of the influence of Zn/Al mass ratio on the creep resistance and tensile properties of As-cast Mg-Zn-Al alloy," *Journal of Alloys and Metallurgical Systems*, vol. 4, pp. 231-245, 2023., <https://doi.org/10.1016/j.jalmes.2023.100033>
- [7] M. O. Esangbedo, B. O. Taiwo, H. H. Abbas, S. Hosseini, M. Sazid, and Y. Fissaha, "Enhancing the exploitation of natural resources for green energy: An application of LSTM-based meta-model for aluminum prices forecasting," *Resources Policy*, vol. 92, pp. 143-152, 2024., <https://doi.org/10.1016/j.resourpol.2024.105014>
- [8] J. L. Guo et al., "Microstructure evolution and constitutive model for Al-Zn-Mg-Cu alloy in hot compression with instantaneously switching strain rates," *Materials Today Communications*, vol. 44, pp. 431-440, 2025., <https://doi.org/10.1016/j.jmrt.2023.08.203>
- [9] D. He, H. Xie, Y. C. Lin, X.-T. Yan, Z. Xu, and G. Xiao, "Microstructure evolution mechanisms and a physically-based constitutive model for an Al-Zn-Mg-Cu-Zr aluminum alloy during hot deformation," *Journal of Materials Research and Technology*, vol. 26, pp. 4739-4754, 2023., <https://doi.org/10.1016/j.jmrt.2023.08.203>
- [10] X. He, X. Xu, X. Xiao, G. Wang, Y. Deng, and Y. Fan, "A simple model revealing the evolution of mechanical properties in Al-Zn-Mg-Cu alloys with a rich Al angle based on CALPHAD," *Journal of Materials Science & Technology*, vol. 227, pp. 241-254, 2025., <https://doi.org/10.1016/j.jmst.2024.12.022>
- [11] X. Jiang, X. Chen, Q. Li, and D. Wang, "First-principles study of the effects of Y and Zn on tensile properties, electronic structure and elastic modulus of magnesium alloys," *Materials Today Communications*, vol. 45, pp. 649-661, 2025., <https://doi.org/10.1016/j.mtcomm.2025.112435>
- [12] S. A. Kareem et al., "Hot deformation behavior of magnesium alloys: A comprehensive review of plastic flow, deformation mechanisms, constitutive modeling and processing maps analysis," *Progress in Engineering Science*, vol. 2, pp. 745-757, 2025., <https://doi.org/10.1016/j.pes.2024.100045>
- [13] S. A. Kareem et al., "Hot deformation behavior of aluminum alloys: A comprehensive review on deformation mechanism, processing maps analysis and constitutive model description," *Materials Today Communications*, vol. 44, pp. 712-723, 2025., <https://doi.org/10.1016/j.mtcomm.2025.112004>
- [14] X. Li et al., "Effect of Cu and Zn on microstructure and mechanical properties of Al-Mg-Si cast alloy," *Journal of Alloys and Compounds*, vol. 1036, pp. 745-758, 2025., <https://doi.org/10.1016/j.jallcom.2025.181688>
- [15] K. Liu, R. Su, G. Li, and Y. Qu, "The influence of secondary aging on the microstructure and corrosion resistance of Al-Zn-Mg-Cu alloy," *Materials Today Communications*, vol. 41, pp. 2154-2168, 2024., <https://doi.org/10.1016/j.mtcomm.2024.111021>
- [16] N. Martynenko et al., "Effect of warm rotary swaging on the mechanical and operational properties of the biodegradable Mg-1 %Zn-0.6 %Ca alloy," *Journal of Magnesium and Alloys*, vol. 13, no. 5, pp. 2252-2266, 2025., <https://doi.org/10.1016/j.jma.2025.03.019>
- [17] E. B. Moustafa, H. D. Natto, E. M. Banoqitah, M. A. Alazwari, A. O. Mosleh, and A. M. Khalil, "Improving the mechanical and dynamic properties of Al-Zn-Mg-Cu based aluminum alloy: A combined approach of microstructural modification and heat treatment," *Journal of Alloys and Compounds*, vol. 1013, pp. 1853-1867, 2025., <https://doi.org/10.1016/j.jallcom.2025.178558>
- [18] A. C. Ozdemir, K. Buluş, and K. Zor, "Medium- to long-term nickel price forecasting using LSTM and GRU networks," *Resources Policy*, vol. 78, pp. 216-230, 2022., <https://doi.org/10.1016/j.resourpol.2022.102906>

- [19] H. Teng et al., "Ultrafine PdMo alloy nanowires mitigate excessive oxygen adsorption to enhance oxygen reduction in Zn-air batteries," *Journal of Colloid Interface Sci*, vol. 699, pp. 1238-1251, 2025., <https://doi.org/10.1016/j.jcis.2025.138273>
- [20] S. Van den Eynde et al., "Forecasting global aluminium flows to demonstrate the need for improved sorting and recycling methods," *Waste Manag*, vol. 137, pp. 231-240, 2022., <https://doi.org/10.1016/j.wasman.2021.11.019>
- [21] C. Wang, M. Guo, J. Zhi, and L. Zhuang, "Greatly improved room temperature formability of Al-Zn-Mg-Cu-Fe alloy sheets via coupling distribution of domains with different strengths," *Journal of Alloys and Compounds*, vol. 1005, pp. 225-238, 2024., <https://doi.org/10.1016/j.jallcom.2024.176249>
- [22] Y. Wu, K. Liu, J. Li, J. Wang, and N. Soboleva, "A review on formation and suppression mechanisms of porosity and cracks in wire arc-directed energy deposition Al-Zn-Mg-Cu alloys," *Journal of Manufacturing Processes*, vol. 148, pp. 173-211, 2025., <https://doi.org/10.1016/j.jmapro.2025.05.017>
- [23] W. Xue et al., "Influence of impurity content on corrosion behavior of Al-Zn-Mg-Cu alloys in a tropical marine atmospheric environment," *Corrosion Science*, vol. 237, pp. 654-667, 2024., <https://doi.org/10.1016/j.corsci.2024.112319>
- [24] Z. Zhang et al., "Improving mechanical properties of Mg-Zn-Nd-Zr alloy by low alloying with Yb and corresponding strengthening mechanisms," *Journal of Materials Research and Technology*, vol. 33, pp. 2023-2034, 2024., <https://doi.org/10.1016/j.jmrt.2024.09.197>